Les Cahiers du GERAD ISSN: 0711–2440

Defragmentation-aware multilayer route and spectrum assignment in elastic optical network

E. Rezaghoilzadeh, S. Kohlert, R. Kashyap, B. Sansò

G–2025–03

January 2025

La publication de ces rapports de recherche est rendue possible grâce au soutien de HEC Montréal, Polytechnique Montréal, Université McGill, Université du Québec à Montréal, ainsi que du Fonds de recherche du Québec – Nature et technologies.

Dépôt légal – Bibliothèque et Archives nationales du Québec, 2025
– Bibliothèque et Archives Canada, 2025

The publication of these research reports is made possible thanks to the support of HEC Montréal, Polytechnique Montréal, McGill University, Université du Québec à Montréal, as well as the Fonds de recherche du Québec – Nature et technologies.

Legal deposit – Bibliothèque et Archives nationales du Québec, 2025
– Library and Archives Canada, 2025

GERAD HEC Montréal
3000, chemin de la Côte-Sainte-Catherine
Montréal (Québec) Canada H3T 2A7

Tél. : 514 340-6053
Téléc. : 514 340-5665
info@gerad.ca
www.gerad.ca

Defragmentation-aware multilayer route and spectrum assignment in elastic optical network

Ehsan Rezaghoilzadeh [a, c]

Scott Kohlert [d]

Raman Kashyap [b, c]

Brunilde Sansò [a, c]

[a] *Department of Electrical and Computer Engineering, Polytechnique Montréal, Montréal, (Qc), Canada, H3T 1J4*

[b] *Department of Engineering Physics, Polytechnique Montréal, Montréal, (Qc), Canada, H3T 1J4*

[c] *GERAD, Montréal (Qc), Canada, H3T 1J4*

[d] *Ciena Corporation, Hanover, Maryland, 21076, United States*

ehsan.rezagholizadeh@polymtl.ca
skohlert@ciena.com
raman.kashyap@polymtl.ca
brunilde.sanso@polymtl.ca

January 2025
Les Cahiers du GERAD
G–2025–03

Abstract : Integrating Optical Transport Networks (OTNs) into multilayer Elastic Optical Networks (EONs) enhances data transmission efficiency but introduces significant challenges in routing and spectrum allocation, particularly when Ethernet connections are encapsulated within OTN payloads. To address these challenges, we develop an Integer Linear Programming (ILP) model tailored for dynamic traffic scenarios to optimize Route and Spectrum Assignment (RSA) in multilayer EONs under OTN constraints. Recognizing the scalability limitations of the ILP model, we propose a novel heuristic algorithm based on a Collapsed Auxiliary Graph (CAG) that abstracts the multilayer network into a single layer. We employ a label-setting approach to solve the constrained shortest path problem on the CAG. This method effectively prevents spectrum interference and controlling latency along demand paths. It also enables fine-tuning of CAG edge weights to implement various traffic engineering policies. Simulation results demonstrate that our heuristic effectively reduces the blocking ratio and improves spectrum utilization while balancing network efficiency and minimizing OTN switching usage. Our findings provide valuable insights into the impact of individual layer configurations on overall network performance, highlighting the effectiveness of our approach in optimizing multilayer EONs with OTN integration.

Keywords : Elastic Optical Networks, traffic grooming, Optical Transport Network, Ethernet over OTN over EON, Route and Spectrum Assignment

Acknowledgements: This work was supported by MiTACS and Ciena Corporation.

1 Introduction

The rapid growth of bandwidth-intensive Internet applications, such as video on demand, is pushing optical networks to their capacity limits, necessitating more efficient data transmission solutions. Traditional fixed-grid wavelength-division multiplexing networks utilize predefined wavelengths to multiplex data streams but lack flexibility in accommodating varying bandwidth requirements [13]. Elastic Optical Networks (EONs) address this limitation by dynamically allocating spectrum to optical transponders based on specific bandwidth needs, allowing adjustments in channel spacing, modulation formats, optical bit rates, and optical reach [3]. However, even though EONs provide spectral flexibility, a mismatch remains between the relatively coarse granularity of optical channels and the finer granularity of Ethernet connections, making traffic grooming a critical tool for improving resource usage and efficiency. Two primary grooming strategies exist in modern optical networks: optical grooming and electrical grooming. Optical grooming utilizes Sliceable Bandwidth Variable Transponders (SBVTs) to manage multiple optical flows efficiently from a single source to various destinations [14]. While promising, optical grooming may require longer paths to combine channels, consuming more spectrum resources and potentially increasing latency. Additionally, it remains largely experimental and is not widely available in commercial equipment.

On the other hand, electrical grooming can be implemented at various network layers, including IP, Ethernet, or the Optical Transport Network (OTN) layer. OTN-based electrical grooming multiplexes Ethernet demands within the OTN framework and transmits them over optical channels, referred to as lightpaths. Additionally, OTN provides the capability for OTN switching, which enables the extraction of a demand from one lightpath and its insertion into another to form a multi-hop path, thus enabling efficient transmission in congested networks or over long distances without regenerating the entire optical channel. It offers lower delay compared to Ethernet switching and enhances performance monitoring through features like Tandem Connection Monitoring (TCM) and advanced Forward Error Correction (FEC) [10]. Integrating the OTN layer into multilayer EONs introduces significant challenges, particularly in routing and spectrum allocation when Ethernet connections are encapsulated within OTN payloads. OTN switching, while beneficial, introduces constraints such as limited switching capacity and specific payload specifications.

In this work, we address the Route and Spectrum Assignment (RSA) problem in multilayer EONs with OTN constraints. We present a framework for integrating OTN over EONs, supporting OTN layer traffic grooming and addressing the OTN constraints. We first develop an Integer Linear Programming (ILP) model for online RSA in multilayer EONs. Although this model can yield an optimal solution, its computational complexity is prohibitively high for large-scale or real-time scenarios.

To overcome scalability challenges, we propose a heuristic algorithm based on a *Collapsed Auxiliary Graph (CAG) model*, designed to reduce the complexity of typical multi-layer Auxiliary Graph (AG) approaches. Unlike existing techniques that may incur excessive computational overhead and spectrum interference, our CAG compresses both optical-layer (e.g., spectrum continuity and contiguity) and OTN-layer (e.g., limited switching capacity, payload specifications) constraints into a unified representation containing only essential nodes and edges.

Furthermore, we employ a *label-setting* algorithm on top of the CAG to solve the constrained shortest path problem. This method not only prevents spectrum interference (i.e., conflicts among newly created lightpaths and extended ones) but also lets us incorporate practical limits, such as the maximum number of hops or the maximum number of new lightpaths per demand. As a result, network operators can balance latency requirements, equipment availability, and cost-efficiency in a more granular way compared to older multi-layer AG solutions.

Building on these methodological advancements, this paper makes the following key contributions (1) we introduce an ILP model that, to the best of our knowledge, is the first to incorporate a probability of blocking formulation for online traffic; (2) we resolve potential spectrum conflicts by using a label-setting algorithm, which also enables controlling network parameters such as the maximum number of

hops; (3) we propose a CAG that unifies all layers while retaining only a necessary subset of nodes, thus improving computational efficiency; and (4) we demonstrate, via simulations, the practical performance benefits of this approach in reducing blocking ratio and enhancing spectrum utilization.

The rest of the paper is organized as follows. Section 2 reviews related research. Section 3 provides an overview of OTN and details the problem. Section 4 presents the ILP model for online multilayer RSA in EONs. Section 5 introduces our CAG model and traffic grooming algorithms. Section 6 discusses simulations and numerical results. Finally, Section 7 concludes the paper.

Table 1: Acronyms and full forms.

Acronym	Full Form
OTN	Optical Transport Network
EON	Elastic Optical Network
ILP	Integer Linear Programming
AG	Auxiliary Graph
CAG	Collapsed Auxiliary Graph
SBVT	Sliceable Bandwidth Variable Transponder
BVT	Bandwidth Variable Transponders
OEO	Optical-Electrical-Optical
TCM	Tandem Connection Monitoring
FEC	Forward Error Correction
RSA	Route and Spectrum Assignment
ODU	Optical Data Unit
ROADMs	Reconfigurable Optical Add-Drop Multiplexers
WSSs	Wavelength Selective Switches
FS	Frequency Slot
O/D	Origin/Destination
PL	Potential Lightpath
EL	Existing Lightpath
EEL	Extendable Existing Lightpath
MinEn	Minimize Energy Consumption
MaxMux	Maximize ODU Multiplexing
MaxSE	Maximize Spectral Efficiency
MinPB	Minimize Probability of Blocking
OPU	Optical Payload Unit
ABP	Access Blocking Probability
KPI	Key Performance Indicator
RL	Reinforcement Learning

2 Related work

Extensive research efforts have been dedicated to tackling the challenges of multilayer routing and spectrum allocation in EONs. A prevalent approach in these studies involves the use of AGs to develop heuristic algorithms for efficiently managing online traffic.

Zhang et al. [21] proposed an AG-based framework to implement various grooming policies, including maximizing spectrum efficiency, minimizing blocking ratio, reducing the number of used transponders, and minimizing energy consumption. They introduced a spectrum reservation strategy to accommodate potential increases in traffic. In their AG model, each block of the available spectrum is represented as an additional layer. Yu et al. [19] introduced a strategy called Traffic Grooming with Spectrum Engineering (TG-SE) for managing online traffic in EONs. Instead of relying on spectrum reservation, this approach leverages spectrum defragmentation. TG-SE employs sliceable transponders and an AG with edge weights dynamically updated for each new connection request, enabling flexible traffic grooming strategies that incorporate both electrical and optical grooming.

To incorporate energy efficiency into Multilayer RSA, Gkamas et al. [5] presented energy-efficient algorithms for multilayer networks, focusing on routing, modulation-level, and spectrum assignment in EONs. They utilized a modified Dijkstra's algorithm to identify non-dominated paths, aiming to

enhance energy efficiency in dynamic network environments. Ghazvini et al. [6] incorporated both electrical and optical grooming in their AG design, featuring multipath routing—an approach not applicable in OTN networks—for spectrum defragmentation. They also utilized adaptive modulation to reduce bandwidth requirements and implemented load balancing for routing. By adjusting edge weights, they employed various traffic grooming plans to improve blocking ratios, spectrum and transponder utilization, and energy efficiency in EONs. Zhu et al. [22] introduced the energy-efficient traffic grooming method for IP-over-fixed/flex-grid optical networks. Their approach employs a two-layer AG with grooming capabilities at both the electrical and optical layers. The AG assigns weights to reflect the relationship between traffic grooming and energy consumption models for IP ports and transponders. Similarly, Costa et al. [3] focused on reducing energy consumption by presenting an AG for both electrical and optical traffic grooming, where each modulation scheme is represented as a separate layer in the AG.

Zhang et al. [20] proposed a three-layered AG approach to solve the RSA problem in SBVT-based EONs. By modifying edge weights, they supported both electrical and optical grooming. Additionally, they introduced the spectrum reservation for each node-pair technique to improve network efficiency and spectrum utilization. Eira et al. [4] presented a technique to enhance multi-period planning in optical networks with SBVTs, enabling the analysis of transport-client layer interactions under various grooming and switching conditions. While their approach considers finite switching capacity, it is primarily limited to static demand scenarios.

Recent advancements have seen the application of machine learning, particularly Reinforcement Learning (RL), in multilayer network planning to manage large-capacity and diverse traffic demands. For instance, Chen et al. [2] introduced Deep RSA, which utilizes an asynchronous advantage actor-critic algorithm to encode the EON state—including network topology, resource availability, and traffic demands—into a high-dimensional vector. Deep neural networks then process this vector to determine optimal routing paths based on spectrum utilization and route-specific metrics. Similarly, Tanaka [17] proposed a RL-based multilayer path planning method that adjusts AG weights to optimize path designs for cost, energy efficiency, and low blocking probability.

While numerous studies have advanced grooming techniques at the optical or electrical layers, fewer have addressed the integration of OTN as a foundational layer with its specific technological requirements. Our work distinguishes itself by precisely accounting for OTN constraints within the multilayer routing and spectrum allocation problem. Moreover, many existing approaches establish multiple new lightpaths between sources and destinations, which can result in spectrum conflicts. We mitigate this issue by employing the label setting method, allowing control over factors such as the maximum number of hops and the maximum number of new lightpath establishments for each demand, thereby managing end-to-end delay and equipment costs by limiting path length and infrastructure needs. These refinements enhance spectrum efficiency and underscore the novelty and practical relevance of our research in addressing critical challenges in multilayer EONs.

To provide a comprehensive overview of the discussed studies and clearly delineate our contributions, we summarize the related work in Table 2.

3 OTN overview

The OTN architecture is structured as a multi-layered system comprising several distinct sublayers [9]. At its foundation is the Optical Data Unit (ODU) sublayer, which acts as the fundamental signal wrapper. This wrapper can encapsulate a single client signal or multiple client signals multiplexed into the Optical Payload Unit (OPU), a process known as OTN multiplexing or electrical grooming [10]. OTN switching facilitates the extraction of a client signal from an ODU on one line card and its insertion into the ODU payload of another line card [7]. Additionally, Reconfigurable Optical Add-Drop Multiplexers (ROADMs) equipped with Wavelength Selective Switches (WSSs) allow for the

Table 2: Summary of related work on traffic grooming in EONs

Ref.	ILP Model	Method	Grooming Layer	Key Contribution
Zhang [21]	No	AG	Elec.	Various grooming policies; spectrum reservation strategy.
Yu [19]	No	AG	Elec./Opt.	Sliceable transponders and spectrum defragmentation.
Gkamas [5]	No	Modified Dijkstra	Elec.	Non-dominated path selection for energy efficiency.
Ghazvini [6]	Yes	AG	Elec./Opt.	Multipath routing for spectrum defragmentation.
Zhu [22]	No	AG	Elec./Opt.	Energy-efficient grooming for IP over optical networks.
Costa [3]	Yes	AG	Elec./Opt.	Reduced energy consumption with multi-layer AG.
Zhang [20]	No	AG	Elec./Opt.	Three-layered AG with node-pair spectrum reservation.
Eira [4]	Yes	AG	Elec.	Multi-period planning in SBVT-enabled networks.
Chen [2]	No	Deep RL	-	Deep RSA for routing, modulation, and spectrum assignment.
Tanaka [17]	No	RL + AG	Elec.	RL-based multilayer path planning.
This Paper	Yes	AG + Label-Setting	Elec.	ILP for dynamic traffic with OTN constraints; mitigates spectrum conflicts and controls path length

dynamic addition, dropping, or bypassing of specific lightpaths [12]. For our study, we assume that all nodes are equipped with OTN switching and ROADM capabilities.

To enhance flexibility on both the client and network sides, OTN introduces FlexOTN technology [8]. On the client side, ODUflex allows for mapping any integer multiple of a foundational tributary slot (time slot), such as ODU0. On the network side, Bandwidth Variable Transponders (BVTs) can adjust their spectral width and modulation formats to tune the capacity of the line-side transponder, enabling the provision of required data rates over specific optical distances [16]. This combination of FlexOTN and BVTs fully leverages the potential of EONs by offering adaptability and efficiency in handling diverse traffic demands.

However, despite these advancements, several challenges persist in OTN technology. One significant issue is the propagation delay and skew that occur when transmitting signals over multiple lightpaths. This problem arises not only across different physical paths but also within the same route, leading to out-of-order bit arrivals. Deskewing techniques, which delay faster paths to synchronize with slower ones, are limited by the capacity of high-speed memory available for buffering. Moreover, constructing transponders capable of managing skew over extensive distances is currently impractical due to technological and economic constraints. As a result, Ethernet demands cannot be split across different lightpaths [10].

Another challenge is the inconsistent availability of OTN switching across network nodes. Not all nodes may have sufficient OTN switching capacity, which is crucial for network flexibility and efficient traffic management. This inconsistency adds complexity to network design and operation, as routing decisions must account for the varying capabilities of individual nodes.

In our research, we address these challenges by incorporating the practical constraints of OTN technology into our solution design. We recognize limitations such as the necessity for single-path routing of Ethernet demands and the limited OTN switching capacity at certain nodes. By integrating these constraints into our models, we aim to develop solutions that are both theoretically robust and practically applicable.

4 ILP model

In this section, we introduce a mathematical model designed to optimize the routing of Ethernet demands across a multilayer optical network. We begin by modeling the multilayer network structure, detailing each layer and its interactions with adjacent layers. Then, we model the Ethernet traffic demands and explain how they are accommodated within this network framework.

4.1 Multilayer network structure

Let $G^k = (V^k, E^k)$ denote a multilayer topology, where k is the layer index. Each V^k represents the set of nodes in layer k, and E^k represents the set of edges (or links) connecting these nodes. These layers cover from the physical fiber infrastructure up to the Ethernet traffic demands, reflecting the hierarchical structure of the network. An illustrative example is provided in Figure 1, which depicts a four-layer network with G^0 representing the physical fiber layer and G^3 representing the Origin/Destination (O/D) Ethernet traffic layer.

At the lowest layer, G^0, the physical network consists of ROADM nodes V^0 connected by optical fiber links E^0. The optical spectrum in this layer is divided into Frequency Slots (FSs), each with a channel width of 6.25 GHz (based on current technology). With a total optical bandwidth of 4.8 THz using the C-band, there are 768 FSs available for assignment to higher-layer connections.

Above G^0, we have the lightpath layer G^1, comprising OTN switches V^1 and lightpath links E^1. Lightpaths in E^1 are established over the physical fiber layer G^0, respecting layer-zero constraints such as spectrum continuity and contiguity. Similar to E^0 links, E^1 links can include parallel lightpaths to accommodate varying demand types and standardized capacities typically found in optical networks.

Next, the tunnel layer G^2 is introduced to model capacity allocation and facilitate the application of the Erlang B formula for blocking probability. Tunnels are represented as edges E^2 within G^2 and are used to determine the total capacity required between O/D pairs for each traffic class, corresponding to standard Ethernet data rates (e.g., 10GE, 100GE, and 400GE). These tunnels are solely for modeling purposes and assist in efficient resource allocation. Each tunnel accommodates one or more demands and exclusively serves its respective traffic class. Due to finite capacity, multiple tunnels may be established for each O/D pair and traffic class to adequately meet their respective demands.

The tunnels E^2 are mapped onto the network of lightpaths in layer G^1. They are routed either directly via an E^1 link or through a multi-hop route involving multiple E^1 links. In scenarios requiring a multi-hop route, sufficient OTN-switching capacity must be available at the intermediate nodes V^1 along the path. This requirement arises because OTN switches at these nodes need to extract the demand timeslots from one lightpath and encapsulate them into another set of timeslots on the subsequent lightpath towards the destination.

A key distinction between E^1 links in G^1 and E^0 links in G^0 lies in timeslot allocation. When establishing an E^2 edge in layer G^1, the timeslots on E^1 links along its path can vary and do not need to be contiguous. In contrast, E^0 links require contiguous timeslots due to the physical constraints of the optical spectrum.

4.2 Modeling Ethernet traffic

At the top layer, G^3, we model the Ethernet traffic demands between O/D pairs. We consider a set S of traffic classes. Each Ethernet demand is generated through a Poisson process with arrival rate λ_s for traffic class s and requires ω_s timeslots. The holding time of each demand is assumed to have an exponential distribution with rate parameter μ_s.

In the context of OTN, a single Ethernet service cannot be split across multiple OTN tunnels. For example, if a service requires 10 timeslots and two available tunnels have capacities of 5 timeslots each, the service request would be refused. Therefore, our model assumes complete sharing among all demands of the same traffic class, while demands of different traffic classes are not mixed over an E^2 edge.

Illustrative examples: To further clarify the multilayer network structure, consider Figure 1a, which demonstrates the encapsulation of an AF tunnel within the G^1 layer. The tunnel employs timeslots 4, 3, and 4 across the lightpaths AB, BE, and EF, respectively. Specifically, the OTN switch at node B

extracts the fourth timeslot from lightpath AB and inserts it into the third timeslot on lightpath BE. This process illustrates how demands are switched at intermediate nodes when multi-hop routing is necessary.

Moreover, Figure 1c shows the routing of the E^1 lightpath AB via a three-hop fiber path AC, CE, and EB within the G^0 graph, utilizing the first three contiguous FSs. Unlike OTN switches, the ROADM nodes at C and E merely redirect the optical signal without Optical-Electrical-Optical (OEO) conversion.

After establishing the structural framework of the multilayer network, we now focus on the formulation of the ILP model designed to optimize the routing and spectrum allocation in this multilayer network.

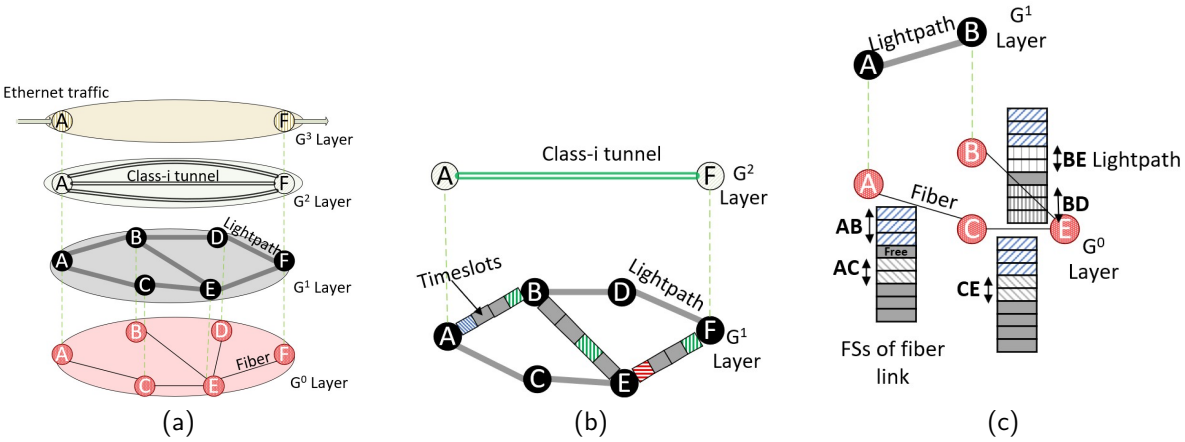

Figure 1: Representation of a multilayer network. Here, G^0 denotes the EON layer, G^1 represents the OTN layer, G^2 signifies class-specific tunnels, and G^3 corresponds to the Ethernet clients. (a) Multilayer network. (b) Mapping tunnel E^2 into lightpath E^1 timeslots. (c) Mapping lightpath E^1 into E^0 FSs.

4.2.1 Parameters and sets

$\mathcal{D}$: Set of all O/D pairs, with each $d \in \mathcal{D}$ as a specific pair.

o_d: Source node of O/D pair d, $o_d \in V^2$.

t_d: Termination node of O/D pair d, $t_d \in V^2$.

λ_s: Arrival rate of s-class Ethernet traffic.

μ_s: Holding time of s-class Ethernet traffic.

ω_s: Number of OTN timeslots needed for s-class Ethernet traffic

D_{mn}: Length of fiber link $mn \in E^0$.

C: Number of FSs in fiber links E^0.

M: Large number, assists the model in some constraints.

T: Set of all operational modes of transponders, each defined by a tuple. The t^{th} tuple includes P_t, representing the number of FSs; L_t, indicating the optical reach; and U_t, denoting the data rate.

R: Maximum number of parallel E^1 links.

Q: Maximum number of parallel E^2 links.

S: Set of traffic classes.

$\bar{B}_{sd}$: Maximum acceptable blocking probability for class s traffic between O/D pair d.

δ: Data rate of an ODU flex timeslot in Gb/s.

Π_n: OTN switching capacity of node $n \in V^1$.

4.2.2 Variables

z_{ijr}: The index of the first FS of the mapping of r^{th} edge $ij \in E^1$ on the optical layer G^0.

x_{sdq}: Number of O/D demand d of traffic class s that can be accommodated by tunnel q.

θ_{sd}: Total number of O/D demand d of traffic class s that can be accommodated by all s-class parallel edges $o_d t_d \in E^2$.

π_n: Processing rate used by OTN switch $n \in V^1$.

$$a_{mn}^{ijr} = \begin{cases} 1 & \text{if the } r^{\text{th}} \text{ edge } ij \in E^1 \text{ encompasses edge} \\ & \quad mn \in E^0,\ r = 1..R \\ 0 & \text{otherwise} \end{cases}$$

$$y_{ijr}^{t} = \begin{cases} 1 & \text{if the transponder type } t \in T \text{ is used for the} \\ & \quad r^{\text{th}} \text{ lightpath } ij \\ 0 & \text{otherwise} \end{cases}$$

$$w_{ijr,i'j'r'} = \begin{cases} 1 & \text{if the start of the first FS occupied} \\ & \quad \text{by the } r^{\text{th}} \text{ link } ij \text{ on the optical} \\ & \quad \text{layer is lower than that occupied} \\ & \quad \text{by the } r'^{\text{ th}} \text{ link } i'j' \\ 0 & \text{otherwise} \end{cases}$$

$$b_{ijr}^{sdq} = \begin{cases} 1 & \text{if the } q^{\text{th}} \ s\text{-class edge } o_d t_d \in E^2 \text{ uses the} \\ & \quad \text{resources of the } r^{\text{th}} \text{ edge } ij \in E^1 \\ 0 & \text{otherwise} \end{cases}$$

l_{ijr}^{sdq}: Number of demands of traffic class s for O/D pair d that are routed through tunnel q over the r^{th} lightpath ij.

4.2.3 Constraints

To ensure the correct and efficient operation of our multilayer optical network, we define a set of constraints categorized according to the network layers and specific operational requirements.

Transponder operational mode constraints: We begin by enforcing that each transponder operates in exactly one operational mode, as specified by Constraint (1). Additionally, we incorporate a dummy transponder mode ($t = 1$) where the FSs P_1 and data rate U_1 are zero, and the optical reach L_1 is set to a large value. This setup allows us to bypass the need to establish all possible edges between every node pair.

$$\sum_{t \in T} y_{ijr}^{t} = 1 \qquad \forall\ ij \in E^1,\ r = 1..R \tag{1}$$

Layer-zero constraints: In the physical fiber layer G^0, we impose Constraints (2) to prevent spectral overlap among lightpaths that share common fiber links. Specifically, Constraints (2) and (3) ensure that if two lightpaths traverse the same fiber, their starting FSs are appropriately separated to avoid interference. Constraints (4) guarantee that each lightpath is allocated the necessary number of FSs as determined by its transponder's operational mode, thereby satisfying the spectrum continuity and contiguity requirements inherent to EONs.

To align the assigned FSs with the available spectrum on each fiber link, we include Constraint (5), which limits the total allocated slots to the fiber's maximum capacity. Equation (6) specifies the flow

conservation constraint to maintain consistent routing of lightpaths in accordance with the network topology. Additionally, Constraint (7) accounts for the optical reach limitations of transponders by restricting the total optical distance of any lightpath to be within the transponder's maximum reach, as determined by the bandwidth and modulation of the transponder.

It is important to note that our model initially assumes a single fiber link between any two neighboring nodes in G^0. To accurately represent scenarios with parallel fiber links, we introduce dummy nodes exclusive to the physical layer. For instance, if two parallel fibers connect nodes A and B, we model one fiber as a direct link between A and B, and represent the second fiber as a path through dummy nodes $A1$ and $B1$. This method allows us to distinguish between parallel links without resource overlap.

$$w_{ijr,i'j'r'} + w_{i'j'r',ijr} \leq 1 \qquad \forall ij, i'j' \in E^1,\ r, r' = 1..R \tag{2}$$

$$w_{ijr,i'j'r'} + w_{i'j'r',ijr} \geq a_{mn}^{ijr} + a_{mn}^{i'j'r'} - 1 \qquad \forall ij, i'j' \in E^1,\ mn \in E^0,\ r, r' = 1..R \tag{3}$$

$$\sum_{t \in T} P_t y_{ijr}^t + z_{ijr} \leq z_{i'j'r'} + M[1 - w_{ijr,i'j'r'}] \qquad \forall ij, i'j' \in E^1,\ r, r' = 1..R \tag{4}$$

$$\sum_{t \in T} P_t y_{ijr}^t + z_{ijr} \leq C \qquad \forall ij \in E^1,\ r, r' = 1..R \tag{5}$$

$$\sum_{mn \in E^0} a_{mn}^{ijr} - \sum_{nm \in E^0} a_{nm}^{ijr} = \begin{cases} 1, & \text{if } m = i \\ -1, & \text{if } m = j \\ 0, & \text{otherwise} \end{cases} \qquad \forall ij \in E^1,\ m \in V^0,\ r = 1..R \tag{6}$$

$$\sum_{mn \in E^0} a_{mn}^{ijr} D_{mn} \leq \sum_{t \in T} L_t y_{ijr}^t \qquad \forall ij \in E^1,\ r = 1..R \tag{7}$$

Layer-one constraints: To linearize the product of variables b_{ijr}^{sdq} and x_{sdq} and obtain the variable l_{ijr}^{sdq}, we apply Constraints (8) and (9). With this linearization, we proceed to manage capacity allocation effectively in the lightpath layer G^1 by establishing Constraint (10). Specifically, we ensure that the total capacity utilized by tunnels (edges in E^2) on any given lightpath does not exceed the lightpath's inherent capacity. Furthermore, we impose limits on the OTN switching capacity at each node through Constraint (12), which is calculated according to Equation (11). Given that traffic both enters and exits an intermediate node, the factor $\frac{1}{2}$ in Equation (11) compensates it.

$$l_{ijr}^{sdq} \leq M b_{ijr}^{sdq} \qquad \forall s \in S,\ d \in \mathcal{D},\ ij \in E^1,\ r = 1..R,\ q = 1..Q \tag{8}$$

$$x_{sdq} - M\left(1 - b_{ijr}^{sdq}\right) \leq l_{ijr}^{sdq} \leq x_{sdq} \qquad \forall s \in S,\ d \in \mathcal{D},\ ij \in E^1,\ r = 1..R,\ q = 1..Q \tag{9}$$

$$\sum_{s \in S, d \in \mathcal{D}, q = 1..Q} l_{ijr}^{sdq} \omega_s \delta \leq \sum_{t \in T} U_t y_{ijr}^t \qquad \forall ij \in E^1,\ r = 1..R \tag{10}$$

$$\pi_n = \sum_{s \in S, q = 1..Q, \{d \in \mathcal{D} | o_d \neq n, t_d \neq n\}} \sum_{r = 1..R, \left\{ij \in E^1 | i = n \ \vee \ j = n\right\}} \frac{1}{2} l_{ijr}^{sdq} \omega_s \delta \qquad \forall n \in V^1 \tag{11}$$

$$\pi_n \leq \Pi_n \qquad \forall\ n \in V^1 \tag{12}$$

Layer-two constraints: For the tunnel layer G^2, we establish Constraint (13) to enforce flow conservation and ensure single-path routing of demands, given that b_{ijr}^{sdq} is a Boolean variable.

$$\sum_{ij \in E^1, r = 1..R} b_{ijr}^{sdq} - \sum_{ji \in E^1, r = 1..R} b_{jir}^{sdq} = \begin{cases} 1, & \text{if } i = o_d \\ -1, & \text{if } i = t_d \\ 0, & \text{otherwise} \end{cases} \qquad \forall i \in V^1,\ d \in \mathcal{D},\ q = 1..Q,\ s \in S \tag{13}$$

Recognizing that resource sharing is exclusive to demands of the same traffic class, we simplify the model by aggregating parallel links between each O/D pair into a single virtual link with a cumulative capacity, as defined by Constraint (14). This aggregation allows us to apply the Erlang B formula, presented in Equation (16) [18], to estimate the blocking probability for each traffic class and O/D pair. To ensure the virtual link capacity meets the desired blocking probability, we precompute values based on the Erlang B formula using the arrival rate and holding time of demands. This approach removes the need to include the non-linear Erlang B function directly in the optimization constraints, as illustrated in Equation (15).

$$\theta_{sd} = \sum_{q=1..Q} x_{sdq} \qquad \forall d \in \mathcal{D},\ s \in S \tag{14}$$

$$\mathcal{B}_{sd}\left(\frac{\lambda_s}{\mu_s}, \theta_{sd}\right) \leq \bar{B}_{sd} \qquad \forall\ d \in \mathcal{D},\ s \in S \tag{15}$$

$$\mathcal{B}_{sd}\left(\frac{\lambda_s}{\mu_s}, \theta_{sd}\right) = \frac{\left(\frac{\lambda_s}{\mu_s}\right)^{\theta_{sd}}}{\theta_{sd}!} \left(\sum_{i=0}^{\theta_{sd}} \frac{\left(\frac{\lambda_s}{\mu_s}\right)^{i}}{i!}\right)^{-1} \tag{16}$$

4.2.4 Objective function

The choice of objective function plays a critical role in optimizing our multilayer optical network. Our primary objective is to minimize the total OTN switching capacity utilized across all nodes in the lightpath layer G^1, as expressed in Equation (17). By reducing OTN switching, we lower energy consumption and network latency while maintaining the desired blocking probability.

$$\min \sum_{n \in V^1} \pi_n \tag{17}$$

Alternatively, other objective functions can be defined to address different optimization goals. For example, minimizing the total number of FSs used across the network emphasizes efficient spectral resource utilization, as formulated in Equation (18).

$$\min \sum_{t \in T, ij \in E^1, r=1..R} P_t y^t_{ijr} \sum_{mn \in E^0} a^{ijr}_{mn} \tag{18}$$

In situations where the maximum acceptable blocking probability $\bar{B}_{sd}$ for each traffic class and O/D pair is not predefined, we extend our optimization to determine this threshold. We formulate a minimax problem, as described in Equation (19), that seeks to minimize the maximum blocking probability across all traffic classes and O/D pairs. The blocking probability of a class s O/D pair d is calculated using the Erlang B function. However, due to the non-linear nature of the Erlang B function, directly solving this minimax problem can be computationally intensive.

$$\begin{aligned} &\min \max_{s \in S, d \in \mathcal{D}} \mathcal{B}_{sd}\left(\frac{\lambda_s}{\mu_s}, \theta_{sd}\right) \\ &\text{s.t.} \quad \text{Constraints (1) to (15)} \end{aligned} \tag{19}$$

To overcome this challenge, we employ an iterative bisection method to approximate the minimum possible blocking probability bound. In each iteration, we test the feasibility of the solution under a specific blocking probability threshold. If a feasible solution exists, we attempt to reduce the blocking probability further; if not, we incrementally increase the threshold.

4.3 ILP model evaluation

To validate the proposed ILP model, we conducted experiments using the Gurobi solver on a simplified network topology consisting of three nodes (A, B, and C) connected by two fiber links (AB and BC), each with a capacity of 64 FSs. The ILP model parameters were set with $R = 4$ and $Q = 8$. We considered Ethernet traffic classes of 10GE, 100GE, and 400GE, each with a traffic load of 1 Erlang, and applied a maximum acceptable blocking ratio of 20%. The transponder operational modes are detailed in Table 5. The table was compiled with data provided by Ciena. We evaluated the ILP model under two objective functions: minimizing the number of used FSs and minimizing OTN switching capacity. We also tested two fiber lengths: 1 and 5. The results are summarized in Table 3.

Table 3: ILP Model Results for different objectives and fiber lengths.

Objective (Fiber length)	**FSs** (Len. 1)	**OTN** (Len. 1)	**FSs** (Len. 5)	**OTN** (Len. 5)
# Lightpaths	5	6	6	7
Total throughput (Gb/s)	4000	3600	3600	3200
FS Usage (%)	89	97	97	98
OTN Switch (Gb/s)	400	0	220	20

The results illustrate the trade-offs between the two objectives. When minimizing the number of used FSs, the model reduces spectral resource consumption, evident from the lower FS usage percentages (89% compared to 97% and 98%). However, this leads to increased OTN switching capacity usage (up to 400 Gb/s), as more traffic is routed through intermediate OTN switches. Conversely, minimizing OTN switching capacity results in higher FS usage and more lightpaths, as the model establishes direct lightpaths to avoid OTN switching.

We also observe that increasing the fiber length from 1 to 5 affects the performance metrics due to the optical reach limitations of transponders. Longer fiber lengths require transponder modes with lower modulation formats, reducing spectral efficiency and leading to higher FS usage and lower total throughput.

Scaling the ILP model to larger networks quickly becomes computationally infeasible. Even adding a single node can result in a problem that the Gurobi solver cannot handle. To overcome this challenge, we need alternative approaches that balance efficiency and solution quality.

5 Heuristic algorithm

To overcome the computational limitations of the ILP model in large-scale networks, we propose a heuristic algorithm. This approach efficiently addresses the optimization problem and adapts to the temporal variability of network properties. Our heuristic leverages the AG concept to optimize multilayer routing and spectrum allocation in EONs, facilitating real-time traffic demands.

First, we define the proposed AG, the foundation of our heuristic. Then, we introduce the Multilayer RSA algorithm that uses the AG to handle new demands. This algorithm has two main parts: assigning edge weights based on traffic engineering policies and a constrained shortest path problem. We then explain these components in detail.

5.1 Collapsed AG:

To efficiently manage new demands in the network, we introduce the Collapsed AG (CAG), which integrates all layers into a single layer. Upon the arrival of a new demand, the CAG is generated based on the set of $\mathcal{K}$ shortest paths determined by optical distance on the G^0 layer. The graph encompasses the demand's source and destination nodes and any intermediate nodes on the $\mathcal{K}$ shortest paths

with adequate ODU switching capacity. This selection process, aimed at minimizing the unnecessary lightpaths, significantly enhances the algorithm's efficiency and scalability, particularly in large-scale network environments.

In the CAG, each node corresponds to a node in the G^1 topology, and the edges represent lightpaths (E^1). To connect nodes in the CAG, we define three types of undirected edges:

Existing Lightpath (EL): They are already established and have enough capacity to accommodate the new demand through ODU multiplexing.

Extendable Existing Lightpath (EEL): ELs that need to be expanded on either the left, right, or both sides of the spectrum to increase OTN payload capacity; otherwise, they're insufficient for the new demand.

Potential Lightpath (PL): Lightpaths that can be created between any pair of nodes in the CAG where neither EL nor EEL exists. These lightpaths require available, continuous, and contiguous FSAs to support the specified demand data rate.

The detailed procedure for constructing the CAG in response to new demands within the network is outlined in Algorithm 1. In the proposed algorithm, several key functions collaborate to dynamically update the CAG in response to new network demands reflecting the current network conditions, such as link capacity, spectrum availability, and operational constraints. The FindKShortestPaths function, leveraging Yen's algorithm [15], identifies the $\mathcal{K}$ shortest paths between demand source and destination nodes. Concurrently, FindParallelELs and FindParallelEELs scan the network for ELs with sufficient capacity and EELs that can be modified to accommodate new demands, respectively. These functions aim to optimize the use of existing network resources by identifying the possibility of multiplexing new demands onto existing infrastructure. Finally, the CheckPL function evaluates the potential for creating new lightpaths, PLs, between node pairs.

Algorithm 1 Dynamic Construction of the CAG in Response to New Demand d.

Input: Ethernet demand d
Output: CAG
Initialization: Invoke FindKShortestPaths(G^0, d) to obtain $\mathcal{P}_\mathcal{K}$
for each path p in $\mathcal{P}_\mathcal{K}$ **do**
  for each node pair (v, v') in path p **do**
    if edge (v, v') exists in CAG **then**
      continue
    end if
    $ELs \leftarrow$ FindParallelELs(v, v')
    if ELs is not empty **then**
      $bestEL \leftarrow$ select the best edge from ELs
      Add $bestEL$ to CAG
    else
      $EELs \leftarrow$ FindParallelEELs(v, v')
      if $EELs$ is not empty **then**
        $bestEEL \leftarrow$ select the best edge from $EELs$
        Add $bestEEL$ to CAG
      else
        $PL \leftarrow$ CheckPL(v, v')
        if PL exists **then**
          Add PL to CAG
        end if
      end if
    end if
  end for
end for
return CAG

To prioritize the use of network resources efficiently, we implement the following scheme for each node pair within the CAG:

- Utilize ELs when available.

- If ELs are not available or sufficient, assess the extendability of ELs (EELs).
- If neither ELs nor EELs are feasible, evaluate the establishment of a PL.

When multiple ELs exist between a node pair, the algorithm employs a best-fit method selecting the EL that most closely meets the demand's bandwidth requirements with minimal excess capacity. For parallel EELs, the best one is chosen based on Access Blocking Probability (ABP) fragmentation reduction before and after the extension of EELs, with details and formula in [1]. Consequently, only one link connects each node pair in the CAG.

In establishing PLs, the algorithm selects the transponder operational mode that either *minimizes spectral usage* or *maximizes data rate*. For *minimum spectral usage*, it chooses the transponder mode with the fewest FSs required to meet the Ethernet demand date rate. For *highest data rate*, it selects the transponder that maximizes data rate to reserve capacity for future demands.

To exemplify the generation of a CAG, let us consider the network illustrated in Figure 2. We construct the CAG for a new demand from source node A to destination node D. The network comprises six ELs where only lightpath BE has adequate capacity for the new demand and node F lacks OTN switching capabilities. We begin by selecting the two shortest paths between nodes A and D. The first path traverses nodes A, B, C, and D, while the second path goes through A, B, E, C, and D. For the first path, we make the following key assumptions:

- The EL between nodes C and D can be extended by adding FSs while no other ELs between different o/d pairs have available FSs for expansion.
- Spectrum availability allows the establishment of new lightpaths solely between node pairs $A-B$ and $A-C$.

With these assumptions, we proceed to construct the CAG by incorporating the EL between nodes $B-C$, which has sufficient capacity, as an EL edge. Additionally, the lightpath between nodes $C-D$, which requires spectral extension to satisfy the demand, is included as an EEL edge. Furthermore, PLs are considered for the node pairs $A-B$ and $A-C$, since sufficient FSs are assumed to be available for establishing new connections. The partial CAG derived from the first path is illustrated in Figure 2b. We repeat this process for the second shortest path $A-B-E-C-D$ to integrate additional nodes and edges, thereby forming the final CAG.

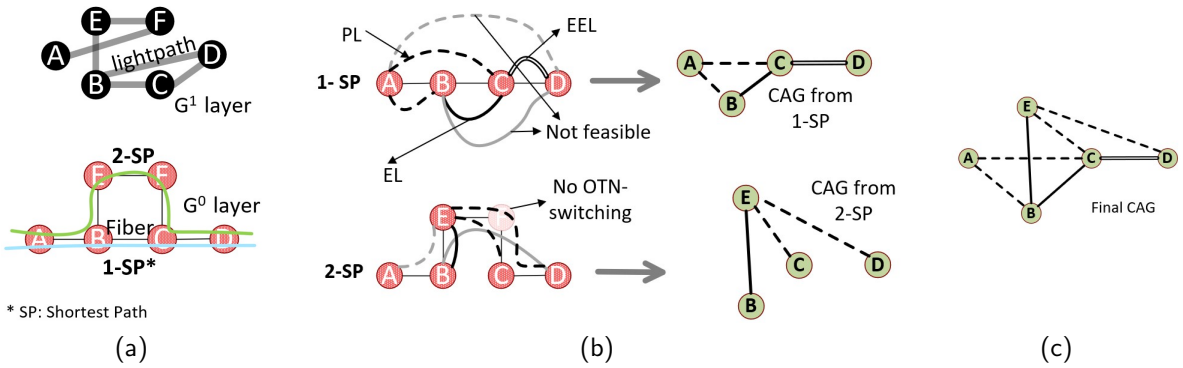

Figure 2: Construction of the CAG for demand from source node A to destination node D. (a) Network topology with six ELs. (b) Building the CAG from two shortest paths. (c) Final CAG.

When incorporating node pairs from each of the $\mathcal{K}$ shortest paths into the CAG, we retain their original routes from the physical network graph G^0 for any PLs. This strategy ensures that PLs do not compete for the same spectral resources on shared fiber links, thereby avoiding conflicts. For example, in the second path, consider the PLs between node pairs $A-E$ and $E-D$. The shortest optical route for $A-E$ is $A-B-E$, and for $E-D$, it is $E-B-C-D$. Both paths share the fiber link between

nodes $B-E$. In a congested network, there might not be enough FSs on link BE to support both PLs simultaneously, even if each could be supported individually. However, by retaining the route of the second shortest path, the proposed routes for these two PLs become $A-B-E$ and $E-F-C-D$, thereby avoiding the conflict on link EB.

5.2 Multilayer RSA algorithm

Following the CAG structure, we now introduce the Multilayer RSA designed to manage new demands. This method is presented in Algorithm 2 and includes two critical components: edge weight assignment based on traffic engineering policies (line 4) and a label setting method (line 5) to solve the constrained shortest path problem. The algorithm begins by constructing the CAG for the incoming demand using the BuildCAG function. After constructing the CAG, the algorithm assigns weights to its edges according to the selected traffic engineering policy presented in Subsection 5.4.

Algorithm 2 RSA Algorithm.

1: **Input:** Ethernet connection request d
2: **Output:** Final status of d (accepted or blocked)
3: $CAG \leftarrow$ BuildAG(d)
4: Assign weights to CAG
5: $p \leftarrow$ LabelSetting(o_d, t_d, CAG)
6: **if** p is not found **then**
7: **return** d is blocked
8: **else**
9: Update the network by adding the demand to ELs, extending EELs, or establishing PLs based on the chosen path
10: **return** d is accepted
11: **end if**

The core of this algorithm is the LabelSetting function, which solves the constrained shortest path problem to identify the most viable path from the source to the destination node within the CAG. If this function, detailed in the following subsection, fails to find a feasible path, the demand is blocked. Conversely, when a viable path is identified, the necessary resources to fulfill the demand are allocated. This includes the utilization of ELs, the extension of EELs, or the establishment of PLs, depending on the chosen routing strategy.

In the following subsections, we explore these components in detail, starting with the label setting method.

5.3 Label setting algorithm

The constrained shortest path problem involves identifying the shortest path within the CAG while considering specific constraints that may affect the feasibility of the path. Notably, recording the path for the O/D pairs does not inherently prevent the possibility of overlapping FSs. While the construction of the CAG includes checks for the feasibility of PLs and EELs, situations may arise where a path becomes infeasible due to simultaneous use. This issue arises when an EL and a PL traverse the same E^0 link, leading to insufficient FSs for both paths. For instance, PL CD and EEL AD in Figure 3 might be individually feasible but cannot coexist when the network is congested.

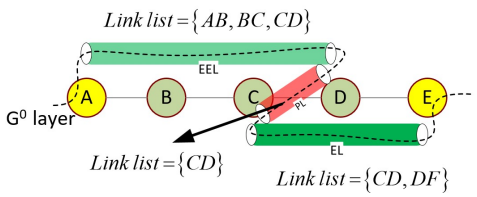

Figure 3: Spectrum overlap between EEL AD and PL CD utilizing link CD in G^0.

To address this, we employ the label-setting Algorithm 3 to solve the constrained shortest path problem. We used forward labeling algorithm which extends labels from the source to the destination [11]. Each label ℓ represents a partial path and encapsulates the following information:

v: Last node of the partial path
τ: Total distance of the partial path
Γ: The list of all E^0 links traversed through the partial path.
η: Number of nodes visited along the partial path.

The first label at the source node o_d is initialized as $\ell_0 = (o_d, 0, \emptyset, 0)$. Given a label ℓ at node v, extending that along the edge (v, v') results in the label $\ell' = (v', \tau_{\ell'}, \Gamma_{\ell'}, \eta_{\ell'})$ and its components are calculated as:

$$\tau_{\ell'} = \tau_\ell + \tau_{vv'} \tag{20}$$

$$\Gamma_{\ell'} = \begin{cases} \Gamma_\ell \cup \Psi_{vv'} & \text{if } vv' \in \text{PLs or EELs} \\ \Gamma_\ell & \text{otherwise} \end{cases} \tag{21}$$

$$\eta_{\ell'} = \eta_\ell + 1 \tag{22}$$

where $\Psi_{vv'}$ is the link list on EON layer to connect lightpath vv' and $\tau_{vv'}$ is calculated in Equation (23). Regarding the Equation (21), We update the set Γ only for labels that extend by PLs and EELs, because ELs are already established and their spectrum usage on E^0 links does not interfere with the allocation of resources for PLs and EELs. The generated label ℓ' is feasible if the set Γ'_ℓ contains unique elements.

The label setting method is optimized through the implementation of elimination and dominance rules. During the label extension process, these rules are evaluated:

Dominance Rules: Label ℓ_2 is dominated by label ℓ_1 if $\Gamma_{\ell_1} \subseteq \Gamma_{\ell_2}$ and $\tau_{\ell_1} \leq \tau_{\ell_2}$. This rule facilitates the early pruning of suboptimal paths in the search process.

Elimination Rules: A label ℓ is discarded prior to further processing if the path length $\eta_{\ell'}$ falls below a specified threshold $\mathcal{H}$. This threshold is a hyperparameter, the optimization of which depends on the prevailing traffic engineering policy.

The pseudocode in Algorithm 3 outlines the operational framework of this label setting algorithm, from initialization through to the iterative evaluation of potential paths, culminating in the identification of the optimal solution. The algorithm initiates by creating the first label ℓ_0 at the source and enqueues this label into a priority queue PQ. The process then enters a loop that iteratively extends and evaluates labels through functions Extend and IsExtendFeasible, based on feasibility and dominance criteria to discover the optimal solution.

5.4 Traffic engineering policies

The traffic engineering policy plays a crucial role in addressing new demands, aiming to optimize network efficiency through enhancing spectrum efficiency, reducing the blocking ratio, minimizing the use of transponders, and conserving energy. One effective way to implement different traffic engineering strategies is by adjusting the edge weights in the CAG. The weight of CAG edge vv', denoted by $\tau_{vv'}$, is calculated using the following equation:

$$\tau_{vv'} = c_0 + I_{vv'} \left(c_0^{\text{new}} + c^{\text{new}} h_{vv'} + c_f \Delta f_{vv'} + c' h_{vv'}^2 + c_u 10^{-u_{vv'}} \right) + (1 - I_{vv'}) \left(c^{\text{old}} h_{vv'} \right) \tag{23}$$

In this equation:

c_0: Constant base cost for each edge.
$I_{vv'}$: Boolean indicating if edge vv' is a new lightpath, PL, or EL/EEL.

c_0^{new}: Cost to establish new lightpaths.

$h_{vv'}$: Number of fiber spans traversed by the lightpath.

c^{new}: Cost component based on optical distance $h_{vv'}$ of a new lightpath.

$\Delta f_{vv'}$: Change in ABP fragmentation across all links due to lightpath establishment.

c_f: Cost component for fragmentation increase $\Delta f_{vv'}$.

c': Cost of squared optical distance; a higher coefficient promotes multiple short lightpaths over a single long one.

$u_{vv'}$: Data rate of the lightpath.

c_u: Cost component for the modulation scheme of a new lightpath; a higher coefficient favors lightpaths with superior modulation schemes for higher data rates.

c^{old}: Cost associated with the optical distance for ELs/EELs.

Algorithm 3 Label Setting Algorithm for Constrained Shortest Path Problem.

Input: Network graph CAG, source node o_d, destination node t_d
Output: Shortest path from o_d to t_d
Initialization: Create the first label ℓ_0 at the source node o_d with initial properties
Initialize a priority queue PQ and enqueue ℓ_0
Set $Solution \leftarrow \emptyset$
while PQ is not empty **do**
  $\ell \leftarrow$Dequeue the top label from PQ
  for each neighbor node i of ℓ **do**
    if IsExtendFeasible(ℓ, i) **then**
      $\ell' \leftarrow$ Extend(ℓ, i)
      if $i = t_d$ and $\tau_{\ell'} < \tau_{Solution}$ **then**
        Update $Solution$ with ℓ'
      else
        Remove Dominated Labels from PQ
      end if
    end if
  end for
end while
return The shortest path stored in $Solution$

By manipulating these coefficients, we can implement various policies. The Minimize Energy Consumption **(MinEn)** policy focuses on reducing power consumption and latency by minimizing the number of OEO conversions at intermediary nodes. The Maximize ODU Multiplexing **(MaxMux)** policy prioritizes the use of ELs/EELs and selects *highest data rate* PLs to maximize the multiplexing of incoming demands. The Maximize Spectral Efficiency **(MaxSE)** policy favors setting up multiple short-distance lightpaths over longer ones to leverage optimal modulation schemes, even if this may increase OTN switching latency. Lastly, the Minimize Probability of Blocking **(MinPB)** policy encourages the establishment of shorter lightpaths to improve spectrum utilization and reduce the requirement for contiguous spectrum allocation over long paths.

These policies are examples, and other policies can be created by adjusting the coefficients in Equation (23). It is also possible to choose the policy per demand based on Quality of Service (QoS) requirements, allowing for flexible and adaptive network management.

Table 4: CAG edge coefficients for different policies.

Policy	c_0	c_0^{new}	c^{new}	c_f	c'	c_u	c^{old}
MinEn	100000	10000	1000	10	0	0	1000
MaxMux	0	1	100	0	0	0	0
MaxSE	0	0	1	0	0	1	1
MinPB	0.000001	0	1000	0	0.001	0	1000

6 Performance evaluation

In this section, we conduct a detailed evaluation of various traffic engineering policies within a multi-layer OTN network. The simulations are performed on the Narval HPC cluster, managed by Calcul Québec within the Digital Research Alliance of Canada, utilizing 100 parallel instances.

The network demands are modeled in granularities of 10GE, 100GE, and 400GE. The simulations account for a FS granularity of 6.25 GHz and 768 FSs per fiber, with the transponders' operational modes shown in Table 5. The network topology, featuring 56 nodes and 72 links, with each node equipped with an ODU multiplexing capacity of 24,000 Gb/s.

We begin our evaluation by assessing the traffic engineering policies, configuring the simulations with $\mathcal{K} = 3$ shortest paths and a maximum hop count of $\mathcal{H} = 5$. Subsequently, we explore the impact of varying these parameters through a hyperparameter study to understand their influence on network performance.

Table 5: Operational modes of the transponder.

Total Capacity (Gb/s)	Modem Bitrate (Gb/s)	Modem Baudrate (Gbaud)	FSs required	Maximum Spans
200	200	95	19	125
300	300	95	19	88
400	400	95	19	54
500	500	95	19	35
600	600	95	19	18
700	700	95	19	9
800	800	95	19	4
100	100	56	12	130
200	200	56	12	61
300	300	56	12	34
400	400	56	12	10
100	100	35	8	75
200	200	35	8	16

Traffic Engineering Policies comparisons: We compare the performance of four traffic engineering policies. The comparison is based on six Key Performance Indicators (KPIs), each chosen for its relevance to network efficiency and performance:

Blocking Ratio: The ratio of blocked Ethernet demands, reflecting the ability of each policy to accommodate incoming traffic.

Average Spectrum Usage %: The percentage of spectral resources utilized under each policy.

Average Hops per Demand: The average number of lightpaths a demand traverses, indicating potential latency implications.

Average OTN Switching: The usage of OTN switching capacity, highlighting operational costs and complexity due to equipment and power consumption.

Average Multi-Demand Lightpath %: The ratio of lightpaths serving multiple demands, indicating the efficiency of traffic aggregation.

Average Lightpath Capacity Usage: The average utilization ratio of lightpath capacities.

Figures 4 to 9 illustrate the comparative performance of different policies according to the previously discussed KPIs. As depicted in Figure 4, the MinPB policy, as expected, demonstrates superior performance in minimizing the blocking ratio. In contrast, the MinEn policy, which consumes more spectrum resources than its counterparts, as detailed in Figure 5, has the highest blocking ratio. Notably, the blocking probability under the MinEn policy surpasses that of MinPB by over 10%, as highlighted in Figure 4.

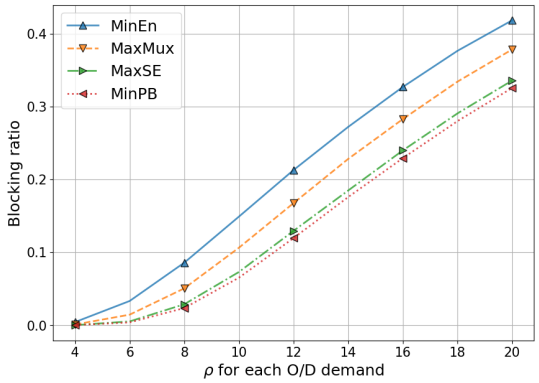

Figure 4: Comparison of blocking ratio across different traffic engineering policies.

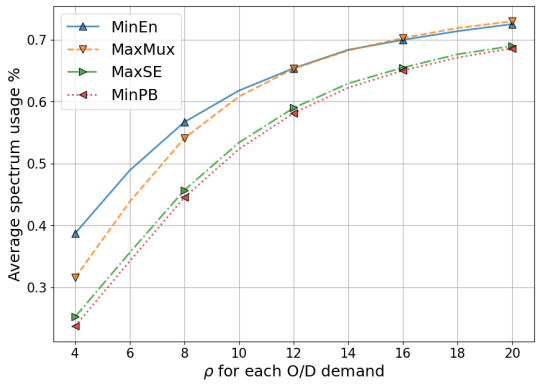

Figure 5: Average spectrum usage percentage by different traffic engineering policies.

The MinPB policy results in the longest path lengths, as illustrated in Figure 6, making it less suitable for low-latency applications. Increased hops per demand imply a higher need for transponders, leading to elevated OTN switching capacity usage. This direct correlation between the average number of hops per demand (see Figure 6) and the average OTN switching (see Figure 7) is clearly demonstrated.

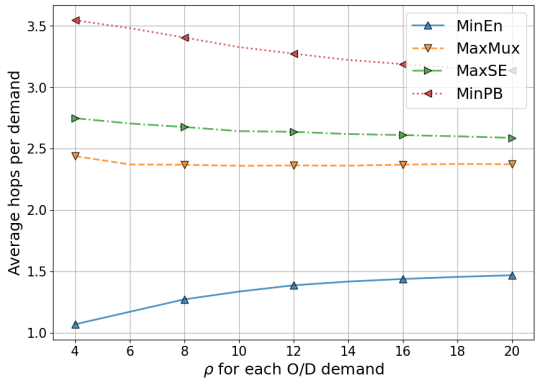

Figure 6: Comparison of average hops per demand across traffic engineering policies.

While OTN switching can reduce the blocking probability, this benefit comes with increased power consumption and delays. This is because higher OTN switching activity, as shown in Figure 7, correlates with reduced spectrum usage (see Figure 5) and a lower blocking ratio (refer to Figure 4).

Moreover, an increase in traffic load leads to higher OTN switching capacity usage. The MaxMux policy, designed to maximize the use of ELs, effectively balances the approaches of MinEn and MinPB.

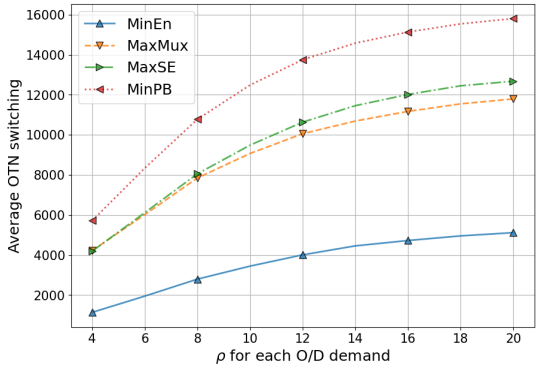

Figure 7: Impact of traffic engineering policies on average OTN switching usage.

The MaxSE policy aims to match the MinPB policy's blocking ratio performance while keeping OTN switching below 30%, as shown in Figure 7. It prioritizes transponder operational modes with the highest modulation schemes to balance network KPIs effectively. Achieving an optimal balance among these metrics presents a significant challenge. Implementing differentiated QoS classes allows for the application of specific policies tailored to the traffic class of each demand. Notably, the MinPB policy demonstrates superior performance in optimizing lightpath capacity usage, as detailed in Figure 9.

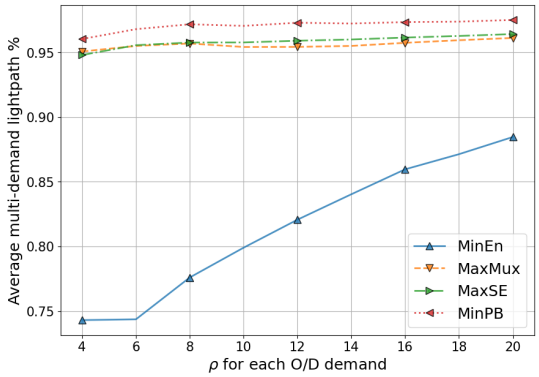

Figure 8: Comparison of traffic engineering policies on the average ratio of multi-demand lightpaths.

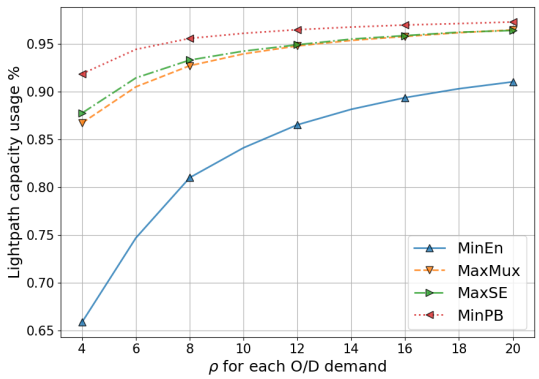

Figure 9: Comparison of traffic engineering policies on average lightpath capacity utilization.

The impact of hyperparameters: The proposed algorithm has key hyperparameters like $\mathcal{H}$, $\mathcal{K}$, and max OTN-switching power. The MinPB policy is used as a reference for evaluating performance. This part examine how variations in OTN-switching power impact network performance. Specifically, Figure 10 shows that increasing OTN-switching power reduces the blocking rate. Concurrently, Figure 12 illustrates improvements in lightpath capacity utilization, whereas Figure 11 indicates that enhanced OTN-switching power results in longer transmission paths. This analysis carefully balances the benefits of increased OTN-switching power against the trade-offs in network path lengths and efficiency.

Figure 13 examines the blocking ratio for three different values of the parameter $\mathcal{K}$. As in previous experiments, the MinPB policy is utilized. Based on this figure, increasing $\mathcal{K}$ from 1 to 3 results in an improvement in the blocking ratio. However, further increasing it to 5 worsens the blocking ratio. The reason is that by routing traffic through longer paths, for example, the fifth shortest path, valuable resources that could be utilized for other demands are consumed. Lastly, Figure 14 examines the performance of the algorithm against $\mathcal{H} = 3, 5, 100$. According to the figure, increasing the $\mathcal{H}$ value from 3 to 5 shows obvious improvement. However, the improvement from 5 to 100 is very negligible. Given that the network has 56 nodes, an $\mathcal{H}$ value of 100 is equivalent to an unrestricted number of hops.

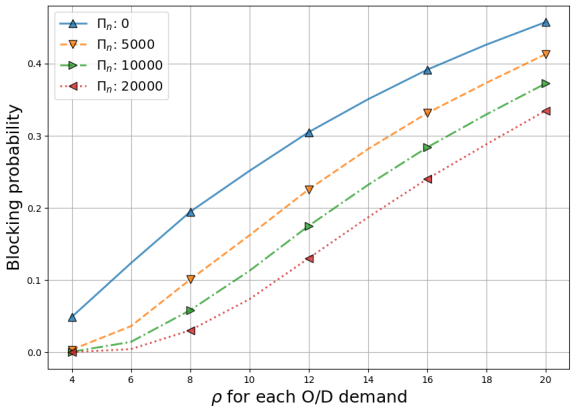

Figure 10: Impact of OTN-switching power on blocking ratio.

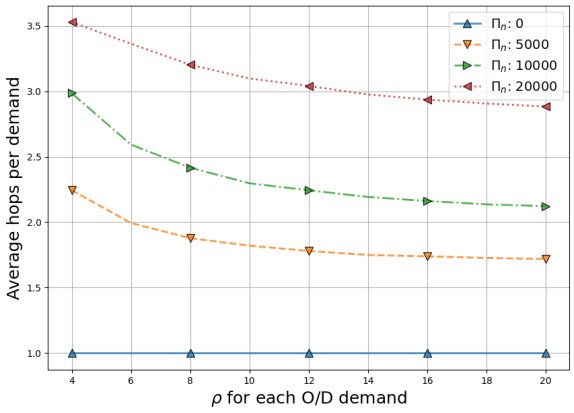

Figure 11: Impact of OTN-switching power on average number of hops.

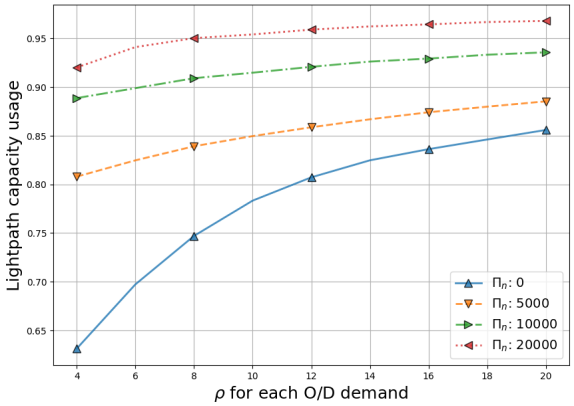

Figure 12: Impact of OTN-switching power on lightpath capacity utilization.

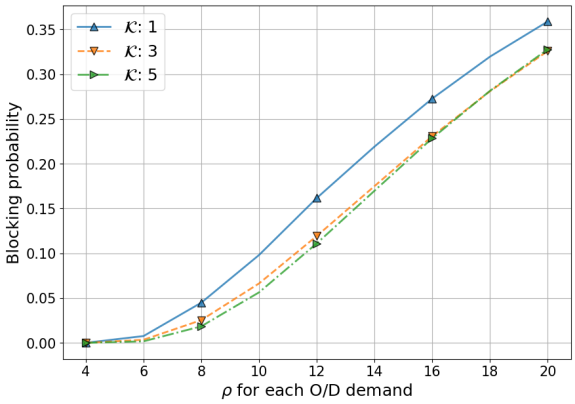

Figure 13: Impact $\mathcal{K}$ on blocking ratio.

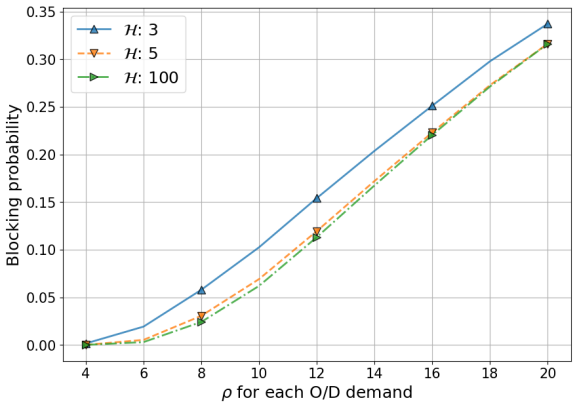

Figure 14: Impact of maximum hops $\mathcal{H}$ on blocking ratio.

7 Conclusions

This paper has presented an extensive study on the integration of the OTN layer within multilayer EONs, focusing on the challenges of routing and spectrum allocation. Our research contributes to the field with the development of an ILP model designed for dynamic traffic scenarios, it tackle the problem with a heuristic approach based on an AG model that we call "collapsed" AG. The CAG model simplifies the three layers of the network into a single layer and resolves the constrained shortest path problem.

Our numerical studies are exhaustive and highlight the impact of individual layer settings on overall network performance. The versatility of our approach is evident in its ability to calibrate CAG edge weights, thereby optimizing network efficiency and maintaining a delicate balance between data blockages and OTN-switching occurrences. The results underscore the potential of our proposed methods in enhancing network efficiency and reliability. The methodologies we have introduced are applicable to the design and operation of OTN over EONs, offering insights into traffic grooming, multilayer RSA, and the management of dynamic traffic patterns.

In conclusion, the strategies and models proposed in this paper hold significant promise for advancing the efficiency and functionality of OTN-EON integrations. Future work could extend these methods to accommodate additional network constraints or to explore the integration of other network layers.

References

[1] Djamel Amar, Esther Le Rouzic, Nicolas Brochier, Jean-Luc Auge, Catherine Lepers, and Nancy Perrot. Spectrum fragmentation issue in flexible optical networks: analysis and good practices. Photonic Network Communications, 29(3):230–243, 2015.

[2] Xiaoliang Chen, Baojia Li, Roberto Proietti, Hongbo Lu, Zuqing Zhu, and S. J. Ben Yoo. Deeprmsa: A deep reinforcement learning framework for routing, modulation and spectrum assignment in elastic optical networks. Journal of Lightwave Technology, 37(16):4155–4163, 2019.

[3] Lucas R. Costa, Italo B. Brasileiro, and Andre C. Drummond. Energy efficiency in sliceable-transponder enabled elastic optical networks. IEEE Transactions on Green Communications and Networking, 5(2):789–802, 2021.

[4] Antnio Eira, Joao Pedro, and Joao Pires. Traffic grooming policies under switching constraints in next-generation transport networks. Journal of Optical Communications and Networking, 9(1):A125–A134, 2017.

[5] Vasileios Gkamas, Konstantinos Christodoulopoulos, and Emmanouel Varvarigos. Energy-aware multilayer flexible optical network operation. In 2015 23rd International Conference on Software, Telecommunications and Computer Networks (SoftCOM), pages 16–21, 2015.

[6] Seyedeh Mina Hosseini Ghazvini, Akbar Ghaffarpour Rahbar, and Behrooz Alizadeh. Load balancing, multipath routing and adaptive modulation with traffic grooming in elastic optical networks. Computer Networks, 169:107081, 2020.

[7] International Telecommunication Union . Characteristics of Optical Transport Network Hierarchy Equipment Functional Blocks. ITU-T Recommendation G.798, International Telecommunication Union, September 2023.

[8] International Telecommunication Union . Flexible OTN Common Elements. ITU-T Recommendation G.709.1, International Telecommunication Union, March 2024.

[9] International Telecommunication Union. Architecture of the Optical Transport Network. ITU-T Recommendation G.872, International Telecommunication Union, March 2024.

[10] International Telecommunication Union - OTN . Interfaces for the optical transport network (otn), g.709 recommendation. ITU-T Recommendation G.709/Y.1331, International Telecommunication Union, June 2020.

[11] Stefan Irnich and Guy Desaulniers. Shortest path problems with resource constraints. In Column generation, pages 33–65. Springer, 2005.

[12] Takuma Kuno, Yojiro Mori, Suresh Subramaniam, Masahiko Jinno, and Hiroshi Hasegawa. Design and evaluation of a reconfigurable optical add-drop multiplexer with flexible wave-band routing in sdm networks. Journal of Optical Communications and Networking, 14(4):248–256, 2022.

[13] Varsha Lohani, Anjali Sharma, and Yatindra Nath Singh. Dynamic routing and spectrum assignment based on the consecutive sub-channels in flexible-grid optical networks. IEEE Access, 10:128354–128365, 2022.

[14] Suzana Miladić-Tešić, Goran Marković, and Valentina Radojičić. Traffic grooming technique for elastic optical networks: A survey. Optik, 176:464–475, 2019.

[15] P.B. Niranjane and S.Y. Amdani. Comparison of variants of yen's algorithm for finding k-simple shortest paths. In 2022 2nd International Conference on Intelligent Technologies (CONIT), pages 1–5, 2022.

[16] Nicola Sambo, Piero Castoldi, Antonio D'Errico, Emilio Riccardi, Annachiara Pagano, Michela Svaluto Moreolo, Josep M. Fàbrega, Danish Rafique, Antonio Napoli, Silvano Frigerio, Emilio Hugues Salas, Georgios Zervas, Markus Nolle, Johannes K. Fischer, Andrew Lord, and Juan P. F.-P Giménez. Next generation sliceable bandwidth variable transponders. IEEE Communications Magazine, 53(2):163–171, 2015.

[17] Takafumi Tanaka. Reinforcement-learning-based path planning in multilayer elastic optical networks [invited]. Journal of Optical Communications and Networking, 16(1):A68–A77, 2024.

[18] Hang Yang, Jing Fu, Jingjin Wu, and Moshe Zukerman. A study of a loss system with priorities. Heliyon, 10(16):e36109, 2024.

[19] Xiaosong Yu, Yongli Zhao, Jiawei Zhang, Jianping Wang, Guoying Zhang, Xue Chen, and Jie Zhang. Dynamic traffic grooming with spectrum engineering (tg-se) in flexible grid optical networks. Optical Fiber Technology, 26:150–156, 2015.

[20] Jiawei Zhang, Yuefeng Ji, Mei Song, Yongli Zhao, Xiaosong Yu, Jie Zhang, and Biswanath Mukherjee. Dynamic traffic grooming in sliceable bandwidth-variable transponder-enabled elastic optical networks. Journal of Lightwave Technology, 33(1):183–191, 2015.

[21] Shuqiang Zhang, Charles Martel, and Biswanath Mukherjee. Dynamic traffic grooming in elastic optical networks. IEEE Journal on Selected Areas in Communications, 31(1):4–12, 2013.

[22] Qingcheng Zhu, Xiaosong Yu, Yongli Zhao, Avishek Nag, and Jie Zhang. Auxiliary-graph-based energy-efficient traffic grooming in ip-over-fixed/flex-grid optical networks. Journal of Lightwave Technology, 39(10):3011–3024, 2021.